Electronic Supplementary Material (ESI) for Physical Chemistry Chemical Physics.

Probing the Electrochemical Capacitance of MXene Nanosheets for High-performance Pseudocapacitors

Xiao Ji,[a] Kui Xu,[a] Chi Chen,[a] Bao Zhang,[a] Yunjun Ruan,[a] Jia Liu,[a] Ling Miao[a] and Jianjun Jiang*[a]

School of Optical and Electronic information, Huazhong University of Science and Technology, Wuhan, Hubei 430074, China

Corresponding author: Ling Miao

Tel:+862787544472

Email: miaoling@mail.hust.edu.cn

Support Information

Section I: Structure of Ti_2CT_2 nanosheets

The structure of Ti_2CT_2 (T = O, F, and OH) nanosheets could be considered as Ti_2CT_2 monolayers stacked following a certain sequence. Hence, the surface structure of Ti_2CT_2 was firstly investigated. Taking the symmetry of Ti_2C into consideration, four major possible configurations of O, F, and OH termination modes were calculated to find the most energy favourable configurations (Figure S 1). For type I, all the O, F, and OH groups are located above the Ti atoms on both sides of the Ti_2C layer; for type II, the groups are placed above the hollow sites between the three neighbouring Ti atoms on both sides of the Ti_2C layer; in type III configuration O, F, and OH groups are oriented above the hollow sites of Ti atoms on one side and point directly toward the C atoms on the other side, forming an asymmetric arrangement on the two sides of the Ti_2C layer; for type IV, all the saturated groups are settle point directly toward C atoms on both side of Ti_2C layer. The corresponding energies of the four considered types of surface structures of Ti_2CT_2 monolayers are list in The results indicate that saturated Ti_2C monolayer are constructed accordingly by saturating the surface under-coordinated Ti atoms with O, F, and OH, respectively.

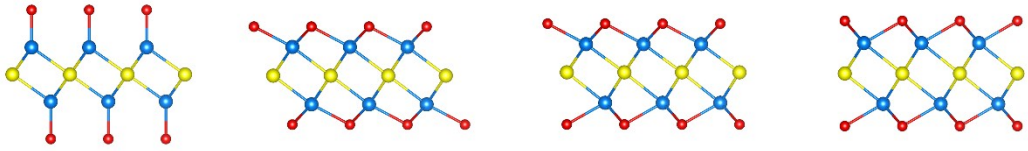

Figure S 1 Four considered types of surface structure of Ti_2CT_2 monolayer.

Table S 1 Energies of the four considered types of surface structures of Ti_2CT_2 monolayers.

Type	Type I	Type II	Type III	Type IV
E [Ti_2CO_2] (eV)	0	-6.29	-5.51	-4.56
E [Ti_2CF_2) (eV)	0	-2.06	-1.85	-1.49
E [$Ti_2C(OH)_2$] (eV)	0	-2.38	-2.28	-2.11

To model the Ti_2CT_2 nanosheets, the configurations interlayer distance of Ti_2CT_2 stack are considered by comparing the relative energy of four possible configurations (Fig. S1). After fully optimization, the schematic show of the most stable structures are illustrated in Figure S 2.

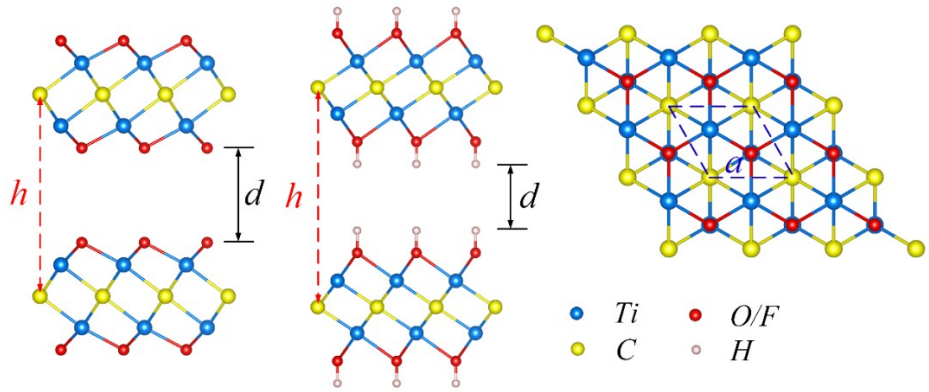

Figure S 2 A schematic showing the crystal structures of Ti2CT2 (T = O, F, and OH) with side view and top view. The Ti, C, O/F and H atoms are represented by blue, yellow, red and white spheres, respectively.

The lattice parameters (*a*), interlayer distances (*h*) and vacuum layer thicknesses between two Ti_2CT_2 layers (*d*) are list in Table S 2.

Table S 2 The calculated lattice parameters (a), interlayer distances (h) and vacuum layer thicknesses between two Ti2CT2 layers (d) for Ti2CT2 nanosheets, respectively.

T	O	F	OH
a (Å)	3.023	3.039	3.047
h (Å)	7.417	7.575	9.801
d (Å)	2.938	2.799	2.969

Section II: Work function of Ti_2CT_x nanosheets

To obtain the work function of Ti_2CT_2 nanosheets respectively, the Fermi energies are aligned to the electron energies in vacuum by calculating the electrostatic potential, as shown in Figure S 3. While calculating the electrostatic potentials of Ti_2CT_2, *c*-axis is set to be 40 Å to get convergence vacuum level. The work function is evaluated by the energy differences between Fermi level and corresponding vacuum level. Here, it is notable that the influence of the number of layer on the work function has not taken into consideration.

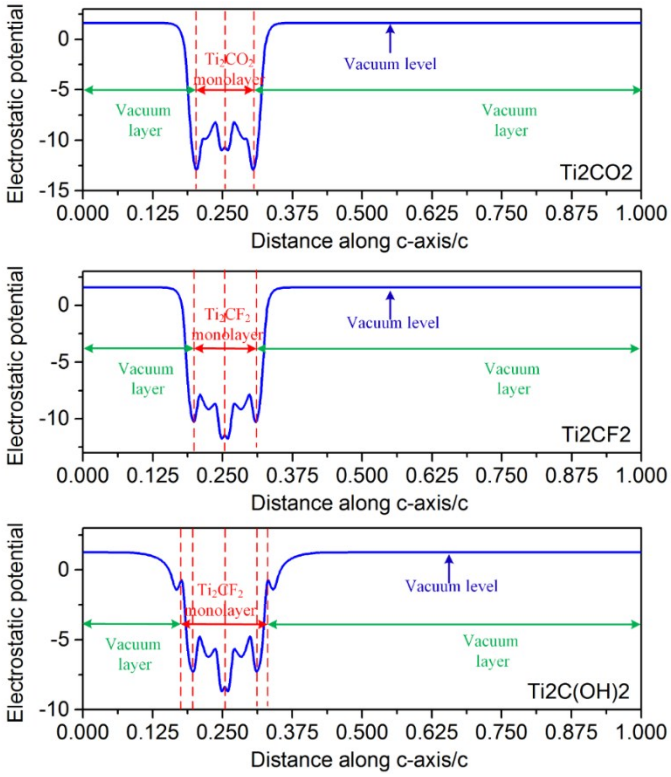

Figure S 3 Calculated electrostatic potential of Ti_2CT_2 monolayer.

The work function of Ti_2CT_2 monolayer is thought to be the same as that of Ti_2CT_2 nanosheets. The detail results are list in Table S 3.

Table S 3 The Fermi level, Vacuum level and work function of Ti_2CT_2 monolayer.

Ti_2CT_2	Fermi level (eV)	Vacuum level (eV)	Work function (eV)
Ti_2CO_2	-4.31	1.53	5.84
Ti_2CF_2	-3.47	1.47	4.94
$Ti_2C(OH)_2$	-0.59	1.26	1.85

Section III: The role of mixture of terminations

Experimental observations support that the as-synthesized MXenes surfaces display a mixture of terminations (-O, -OH, and -F terminations).[1-3] But little effort has been dedicated to understand the complex surface chemistry of MXenes and only a limited number of experimental results can be found. The results show that the distribution of terminal species attached on both sides of bare MXenes is random and non-periodic, which makes enormous difficulties to propose relevant theoretical models.

Heretofore, two-generation theoretical models of MXenes have been used in recent theoretical works. The first-generation models have not taken surface terminations into consideration.[4, 5] The second-generation models assumed uniform coverage of MXene surface with certain functional groups (pure -O, -OH, or -F terminations).[6-8] Recent theoretical works on MXenes are mostly using the second-generation models. The models have not kept in pace with the experimental results, but it is a good way to study the effect of termination on MXenes. Interestingly, a recent work has described and benchmarked a novel way of modeling layered materials (Ti_3C_2-based MXenes) with real interfaces against experimental data.[9] But this model has not been promoted and it is difficult to investigate the role of different terminations.

Herein, in order to study the electrochemical performance of Ti_2C-based MXenes with mixed terminations, Ti_2C-O/OH, Ti_2C-F/OH, Ti_2C-O/F, and Ti_2C-O/F/OH are taken into consideration, as illustrated in Figure S 4. The termination groups are distributed randomly at the ratio of 1:1 or 1:1:1, respectively.

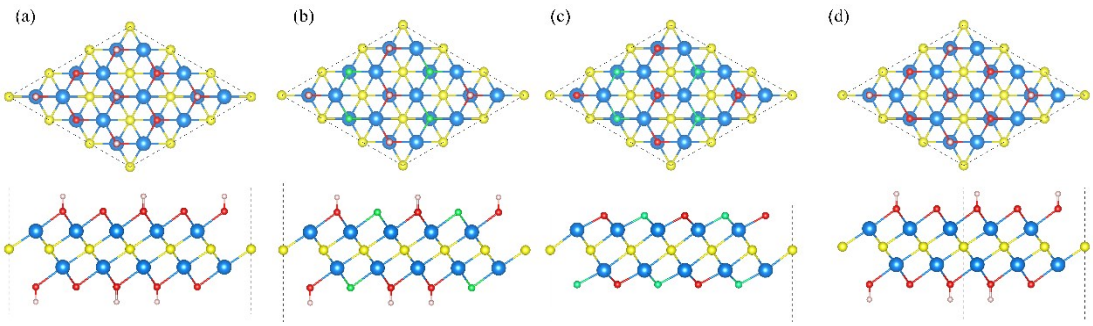

Figure S 4 Top and side view of the Ti2C with mixed terminations: (a) Ti2C-O/OH, (b) Ti2C-F/OH, (c) Ti2C-O/F, and (d) Ti2C-O/F/OH. The blue, yellow, red, and white spheres represent the Ti, C, O, and

H atoms, respectively.

Firstly, the work functions of mixed terminated Ti_2CT_x are listed in Table S 4, by calculating the electrostatic potential (Figure S 5). The work functions of Ti_2CT_x are between/among that pure terminated Ti_2CT_2 (T = O, F, and/or OH). Furthermore, the work function also depends on the configuration of terminated groups. It indicates that the variety and the configuration of terminations will affect the stability and the electrochemical performance of Ti_2CT_x nanosheets.

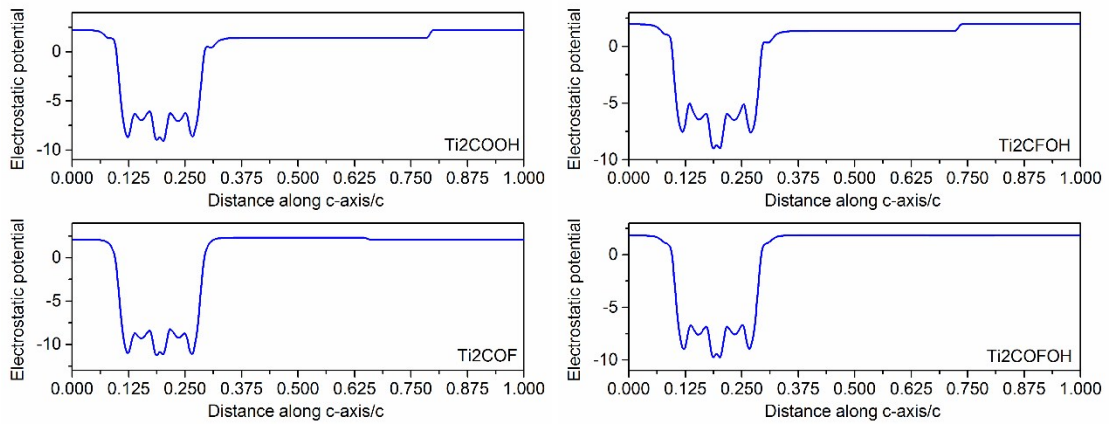

Figure S 5 Calculated electrostatic potential of considered Ti2CTx monolayer.

Table S 4 Fermi level, vacuum level (along +c and –c axes) and relevant work function of Ti2CTx monolayer.

Ti_2CT_x	Fermi level (eV)	Vacuum level (eV)		Work function (eV)	
		+c	-c	+c	-c
Ti_2C-O/OH	-1.39	1.40	2.22	2.79	3.60
Ti_2C-F/OH	-0.74	1.36	1.95	2.11	2.70
Ti_2C-O/F	-3.58	2.31	2.09	5.89	5.68
Ti_2C-O/F/OH	-1.90	1.85	1.83	3.75	3.73

Secondly, PDOS and integral DOS of ***d***-orbitals of Ti-atoms in Ti_2CT_2 and Ti_2CT_x are taken into comparison (Figure S 6). The ***d***-orbital of Ti-atom in Ti_2CT_x have similar distribution to that in Ti_2CT_2. And according to PDOS near Fermi level, the charge-storage capability of Ti-atoms (bonded with O, F, and OH) is smaller than that in

Ti_2CO_2 but larger than that in Ti_2CF_2 and $Ti_2C(OH)_2$.

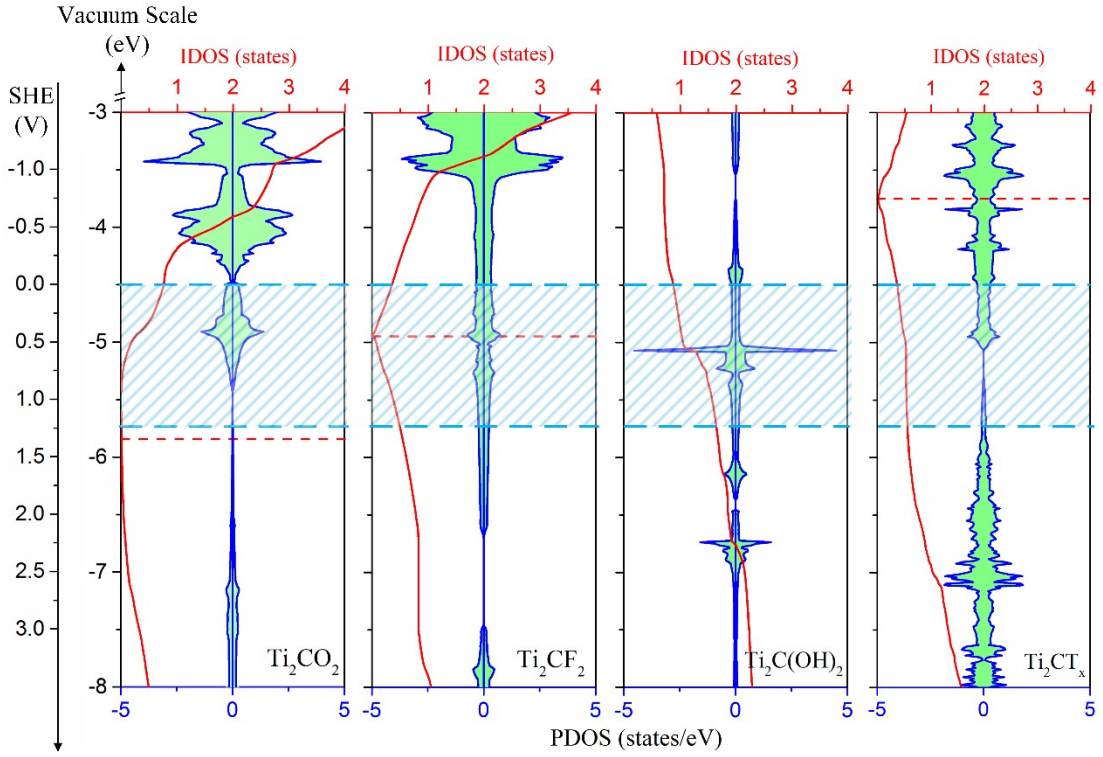

Figure S 6 PDOS and integral DOS of ***d***-orbitals of Ti atoms in Ti_2CT_2 (T = O, F, and OH) and Ti_2CT_x nanosheets shown on the vacuum scale and with respect to SHE reference. The dash lines indicate Fermi level positions of Ti_2CT_2 nanosheets. The blue regions represent electrolyte window.

Finally, the mixed terminations play an important role in deciding the stability in aqueous electrolyte and the charge-storage capability of MXenes according to our calculation. Generally, the instability of pure terminated Ti_2C-MXenes drives the mixture of the terminations, which in return, changes the electrochemical performance of Ti_2C-based MXenes.

The approach we used here is difficult to get the accurate value of electrochemical performance of MXenes with mixed terminations. However, the theoretical work presented in our manuscript could give a comprehension in atomic level to the electrochemical performance of Ti_2CT_x nanosheets.

Section IV: Total density of states of Ti_2CT_2 nanosheets

The electronic conductivity of electrode material, which matters the rate performance and transfer resistance, is a key factor of determining the performance of electrochemistry capacitor. To evaluate the electronic conductivity of Ti_2CT_2 nanosheets, the total density of states of Ti_2CT_2 are depict in Figure S 7. The results show that Ti_2CO_2 nanosheets preserve the semiconducting behaviour with a narrow band gap of about 0.12 eV while the others are showing metallic behaviour. The narrow band gap or metallic behaviour indicates that Ti_2CT_2 nanosheets offer an intrinsic advantage as promising electrochemistry capacitance materials.

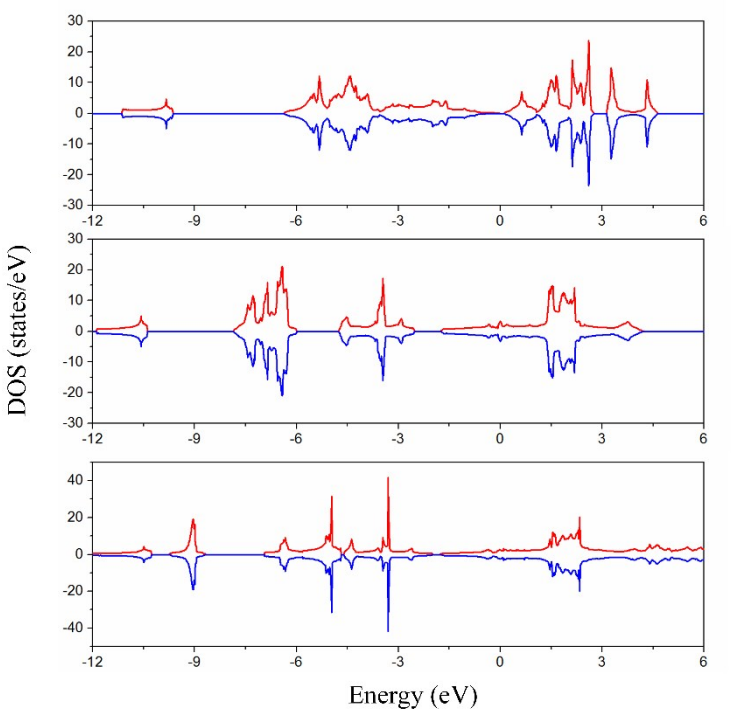

Figure S 7 Total DOS for Ti_2CO_2, Ti_2CF_2 and $Ti_2C(OH)$ nanosheets, respectively. The Fermi level is chosen as 0 eV.

Section V: Na ions adsorption sites in Ti_2CT_2 nanosheets

Three types of sites with high symmetry in the Ti_2CT_2 nanosheets are taken into account: the C, Ti, and T sites. For C sites, the Li ion absorbs on the top of C atoms while for Ti sites, the Li ions is placed on the top of Ti atoms. As for T sites, the Li ion is designed on the top of T (T = O, F, and OH) atoms, as illustrated in Figure S 8.

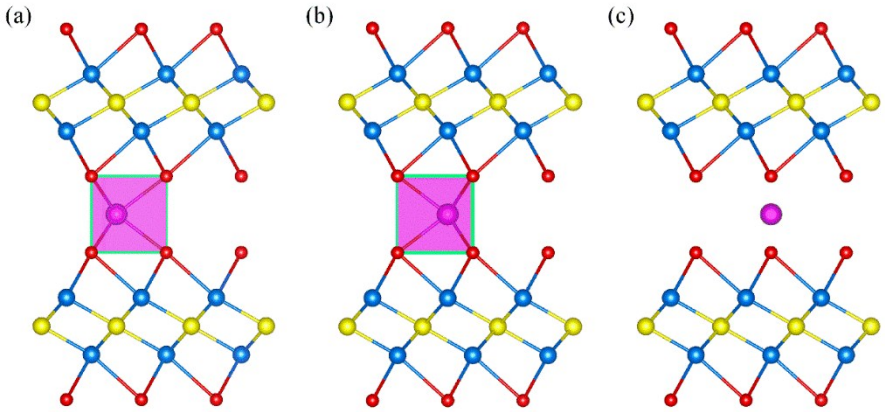

Figure S 8 Three considered Na ion adsorption types of sites in the Ti2CT2 nanosheets, (a) C sites, (b) Ti sites, (c) T sites.

The calculated results are listed in Table S 5. For the Ti_2CT_2 nanosheets, C site are the most energy favorable for Na ion adsorption. Ti_2CO_2 and Ti_2CF_2 nanosheets with the Na ion binding energies of -2.35 and -1.39 eV, respectively, indicating their energy suitability for Na ion adsorption. And after fully relaxed, the Na ion on the top of T site is optimized to C site for Ti_2CO_2 and $Ti_2C(OH)_2$ nanosheets.

Table S 5 The calculated binding energies for three types of sites in Ti_2CT_2 nanosheets.

Ti_2CT_2	C	Ti	T
Ti_2CO_2	-2.35	-2.15	-
Ti_2CF_2	-1.39	-1.04	-1.20
$Ti_2C(OH)_2$	0.44	1.18	-

Section VI: DOS of Na intercalated Ti_2CO_2 and Ti_2CF_2 nanosheets

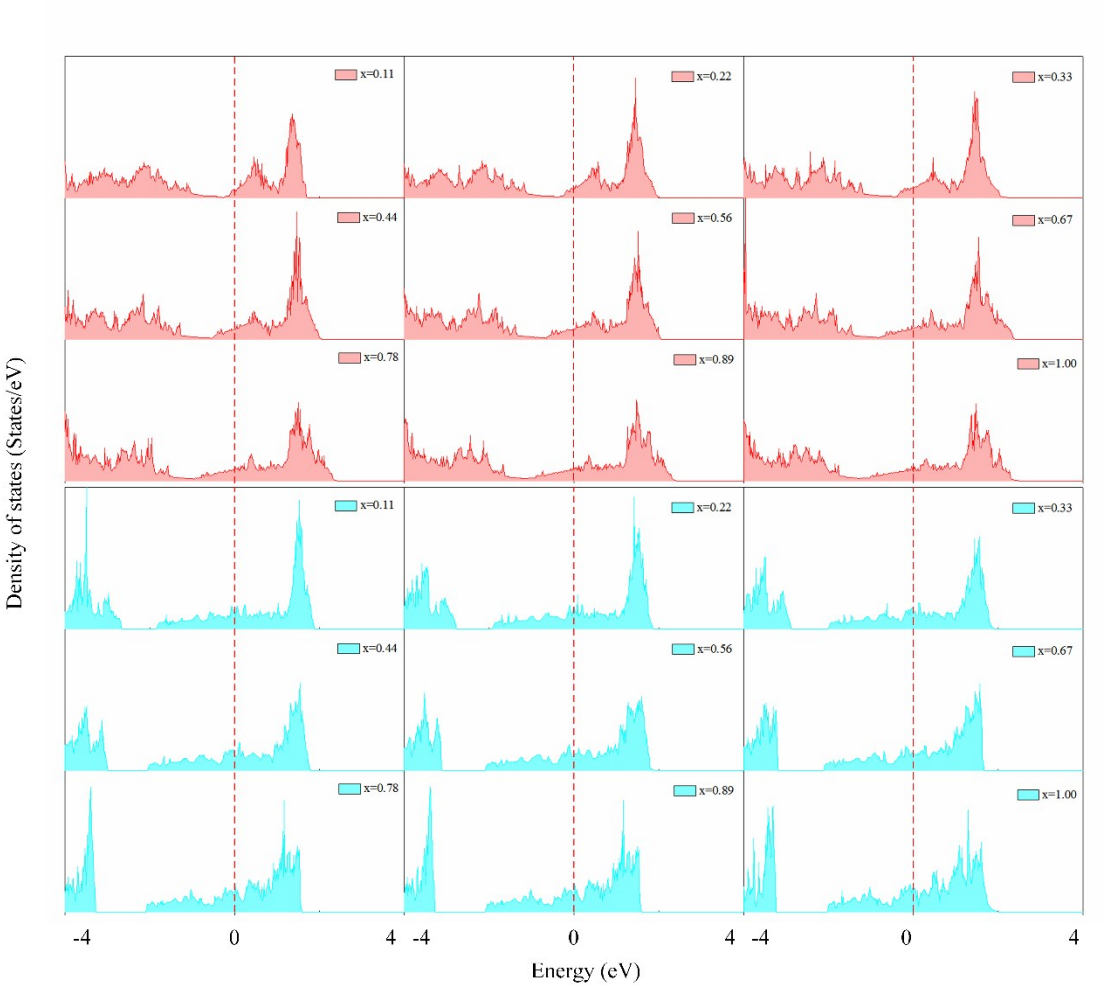

Figure S 9 The calculated DOS of $Ti_2CO_2Na_x$ and $Ti_2CF_2Na_x$ nanosheets at different Na concentration.

Section VII: Considered pathways for Na ions diffusion in Ti_2CO_2 and Ti_2CF_2 nanosheets

Considering the high symmetry of the Ti_2CT_2 nanosheets, three possible pathways between the two nearest neighbouring Na adsorption sites are studied. The results show that ions tend to migrate along the C-Ti-C pathway: Na ion moves from the site on top of C atoms to the one on top of Ti atoms and then to the nearest neighbouring C atoms for both Ti_2CO_2 and Ti_2CF_2 nanosheets, respectively. The C-C pathway allows Na ion migration directly from C site to the nearest C site. But the results show that Na ion is automatically optimized to the C-Ti-C pathway. And for C-T-C pathway, the energy barriers are high for both C-O-C and C-F-C.

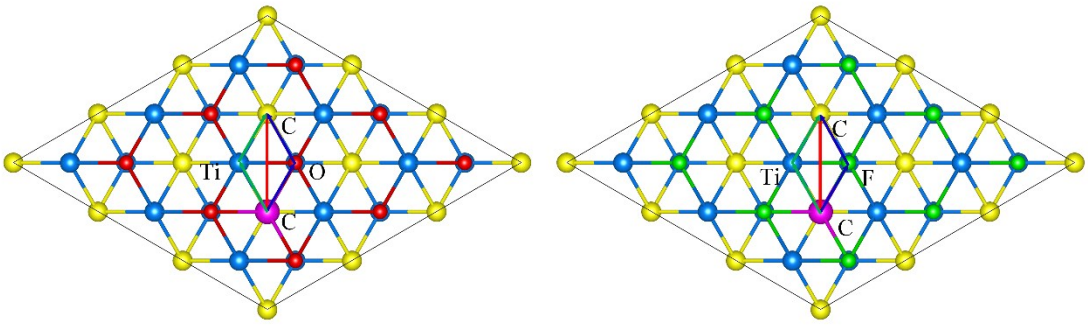

1. X. Wang, X. Shen, Y. Gao, Z. Wang, R. Yu and L. Chen, *J. Am. Chem. Soc.*, 2015, **137**, 2715-2721.
2. J. Halim, K. M. Cook, M. Naguib, P. Eklund, Y. Gogotsi, J. Rosen and M. W. Barsoum, *Appl. Surf. Sci.*, 2016, **362**, 406-417.
3. X. Wang, S. Kajiyama, H. Iinuma, E. Hosono, S. Oro, I. Moriguchi, M. Okubo and A. Yamada, *Nat. Commun.*, 2015, **6**, 6544.
4. S. Zhao, W. Kang and J. Xue, *J. Phys. Chem. C*, 2014, DOI: 10.1021/jp504493a, 140701073355000.
5. D. Er, J. Li, M. Naguib, Y. Gogotsi and V. B. Shenoy, *ACS Appl. Mater. Interfaces*, 2014, **6**, 11173-11179.
6. Y. Xie, M. Naguib, V. N. Mochalin, M. W. Barsoum, Y. Gogotsi, X. Yu, K. W. Nam, X. Q. Yang, A. I. Kolesnikov and P. R. Kent, *J. Am. Chem. Soc.*, 2014, **136**, 6385-6394.
7. J. Hu, B. Xu, C. Ouyang, S. A. Yang and Y. Yao, *J. Phys. Chem. C*, 2014, **118**, 24274-24281.
8. Q. Tang, Z. Zhou and P. Shen, *J. Am. Chem. Soc.*, 2012, **134**, 16909-16916.
9. H.-W. Wang, M. Naguib, K. Page, D. J. Wesolowski and Y. Gogotsi, *Chem. Mater.*, 2015, DOI: 10.1021/acs.chemmater.5b04250.